Scanning Tunneling Microscopy Observation of a Square Abrikosov Lattice in $LuNi_2B_2C$

Y. De Wilde, M. Iavarone,* U. Welp, V. Metlushko, A. E. Koshelev, I. Aranson,† and G. W. Crabtree
Material Science Division-Science and Technology Center for Superconductivity, Argonne National Laboratory, Argonne, Illinois 60439

P. C. Canfield
Ames Laboratory and Department of Physics and Astronomy, Iowa State University, Ames, Iowa 50011
(Received 16 January 1997)

We present scanning tunneling microscopy measurements of the (001) surface of a $LuNi_2B_2C$ borocarbide single crystal at 4.2 K. In zero field, the conductance versus voltage characteristics recorded at various locations on the sample reproducibly provide a gap value of 2.2 meV. In a magnetic field of 1.5 and 0.375 T, the recordings of the conductance as a function of position reveal a regular square vortex lattice tilted by 45° with respect to the crystalline a axis. This unusual result is correlated with an in-plane anisotropy of the upper critical field $H_{c2}^{\parallel}(45°)/H_{c2}^{\parallel}(0) = 0.92$ at 4.2 K and is analyzed within the framework of Ginzburg-Landau theory. [S0031-9007(97)03335-8]

PACS numbers: 74.60.Ge

The scanning tunneling microscope (STM) is a powerful probe of the real space structure of the vortex lattice (VL) of type-II superconductors. Most other techniques, such as magnetic force microscopy [1], Bitter decoration [2], and neutron scattering [3], are sensitive to magnetic contrast on the scale of the London penetration depth λ and are therefore limited to low magnetic fields. STM, in contrast, is sensitive to the local density of states on the much smaller scale of the coherence length ξ and can image vortices even at high fields, where the vortex spacing is smaller than λ. So far, surface quality has limited the observation of vortices by STM to two materials: $NbSe_2$, which presents clean atomically flat surfaces [4–7], and crystals of YBCO grown in special $BaZrO_3$ crucibles [8].

Although the VL forms a hexagonal structure for isotropic superconductors in the absence of pinning [9,10], many deviations from this symmetry have been found, generally associated with anisotropic uniaxial character or pinning by extrinsic defects. A distorted hexagonal symmetry and vortex chains were predicted and observed by Bitter decoration [11], neutron scattering [12], and STM [8] in YBCO and BSCCO along with sawtooth VLs, hexatic lattices, order-disorder transitions, intrinsic pinning, and pinning by twin boundaries. Analogous features were found in $NbSe_2$ by STM [5,7] and Bitter decoration [11].

On the low T_c materials Nb and Pb-Tl, hexagonal, distorted hexagonal, and square VLs, depending on the crystal orientation, were observed by Bitter decoration [13,14] and neutron scattering experiments [15]. A gradual phase transition in Pb-Tl(111) of the VL from hexagonal to square for increasing field was observed and explained by an attractive interaction between the vortices when the vortex spacing is of the order of the coherence length in this low κ material [16,17]. In recent neutron scattering experiments [3] a square VL which transforms to hexagonal at very low fields [18] was observed in an $ErNi_2B_2C$ single crystal. This compound belongs to the recently discovered borocarbide family [19,20] and exhibits an antiferromagnetic ordering which was shown to directly influence the VL [3].

To avoid any possible coupling between magnetic ordering and the VL, we performed STM investigations on $LuNi_2B_2C$ which has the same tetragonal structure as $ErNi_2B_2C$ [21] but has no local magnetic moments. We measure a gap of 2.2 meV at 4.2 K. Our results provide the first vacuum tunneling spectra and STM images of the vortex structure in the borocarbide family. $LuNi_2B_2C$ is the third material, after $NbSe_2$ and YBCO, in which STM images of the vortex lattice have been observed. We find a square VL at 0.375 and 1.5 T, contrary to the hexagonal VL expected in isotropic superconductors in the absence of pinning. The square VL is rotated 45° with respect to the (100) crystal direction, as also found in $ErNi_2B_2C$ [3]. An anisotropy of the Fermi surface, an anisotropic magnetoelastic coupling, and a gap anisotropy have been suggested as three mechanisms which could stabilize a square VL [15]. Regardless of the microscopic origin of a square VL, it can be analyzed phenomenologically using a simple extension of the Ginzburg-Landau (GL) approach. The GL theory is only applicable near T_c which does not allow direct comparison with our STM data. Nevertheless, we apply this approach to determine the range of stability of the square VL in the H-T plane and to establish its correlation with an in-plane anisotropy of H_{c2}.

The experiments were performed on a $LuNi_2B_2C$ single crystal grown by the high temperature flux method using Ni_2B as a solvent [22]. The crystal is a platelet of typical size 2 mm × 2 mm × 0.5 mm; the largest area is normal to the c axis of this tetragonal system [21]; all our STM measurements were done on this surface. SQUID magnetometry was used to measure the zero field critical

temperature T_c of 15.8 K, and the upper critical field H_{c2} at 4.5 K of 5.7 T, for a field applied along the c axis.

The measurements were performed with a home built low temperature STM operating in a helium exchange gas at 4.2 K. In order to obtain a clean surface, the sample was chemically etched in a solution of HCl-HNO_3 (3-1) [23] prior to mounting into the STM. The tip was made of a PtIr wire sharpened mechanically with scissors.

The surface roughness estimated from STM scans in the topography mode over a scale of 4000 Å × 4000 Å is less than 10 Å. Vacuum tunneling was verified by the reproducibility of both the topographic and spectroscopic data recorded over the same area at various tunneling resistances. The differential conductance dI/dV vs V curves were recorded using the standard lock-in technique with a small ac modulation superimposed on the slowly varying bias voltage while the feedback loop was interrupted. The amplitude of the ac modulation was fixed at 0.4 mV peak-to-peak, i.e., a factor of 3 smaller than the intrinsic thermal broadening ($\approx 3.5 k_B T$) of the spectra at 4.2 K.

Figure 1 shows a typical dI/dV vs V spectrum recorded at $H = 0$ and normalized by a slightly quadratic background obtained above H_{c2}. The spectral features shown in this figure are highly reproducible over the entire crystal surface. The value of the gap was estimated by fitting the experimental curves to the standard theoretical expression of the tunneling conductance [24], evaluated at the temperature of the measurements, and a smeared version of the Bardeen-Cooper-Schrieffer (BCS) density of states [25]:

$$N(E) = \mathrm{Re}\{|E - i\Gamma|/[(E - i\Gamma)^2 - \Delta^2]^{1/2}\}, \quad (1)$$

where E is the energy, Δ the superconducting gap and Γ the broadening parameter. The best fit gives $\Delta = 2.2$ mV and $\Gamma = 0.4$ mV. Using the bulk T_c, we obtained a ratio $\frac{2\Delta}{k_B T_c} = 3.2 \pm 0.1$, where the error is due primarily to the width of the superconducting transition. This implies weak-coupling superconductivity in $LuNi_2B_2C$. The gap has been measured previously by point-contact tunneling on polycrystals and single crystals, and by break junctions [26]. These gap values vary widely depending on the type of measurements and, in some cases, with location in a single sample. In contrast, our STM-determined gap values vary remarkably little with location, substantially increasing the precision of the measurement.

In a magnetic field, the vortices are imaged by recording the spatial variations of the lock-in signal, directly proportional to the differential conductance, while the tip is scanning over the sample surface with a constant bias voltage $V_b = 3$ mV. At this bias voltage, the differential conductance is maximum over a superconducting region (Fig. 1) and is expected to decrease when the tip passes over a vortex core. Figure 2(a) represents a gray-scale image of the differential conductance over an area of 2900 Å × 2900 Å for a magnetic field of 1.5 T (field cooled) perpendicular to the sample surface. Figure 2(b) corresponds to an area of 1700 Å × 1700 Å. This figure is the average of all the regions of Fig. 2(a) which show a correlation higher than 99% with an initial kernel chosen in the central area of Fig. 2(a). A square lattice is clearly observed with a lattice constant a_0 equal to 370 Å ± 10 Å, in good agreement with $(\frac{\Phi_0}{B})^{1/2}$ expected for a square lattice. In a field of 0.375 T a similar lattice structure was observed with a spacing consistent with the applied magnetic field. In each case the flux lattice is rotated by 45° with respect to the crystalline a axis, measured by Laue scattering. This is consistent with the recent observation of the square VL in $LuNi_2B_2C$ using neutron scattering [27].

Figure 3 shows a set of four dI/dV vs V characteristics recorded in a field of 0.375 T at various distances from the center of a vortex. No conductance peaks related to localized quasiparticle states in the core [4,6] are observed. With a residual resistivity $\rho = 3\ \mu\Omega$ cm, the electronic mean free path l is estimated [28] to be of the

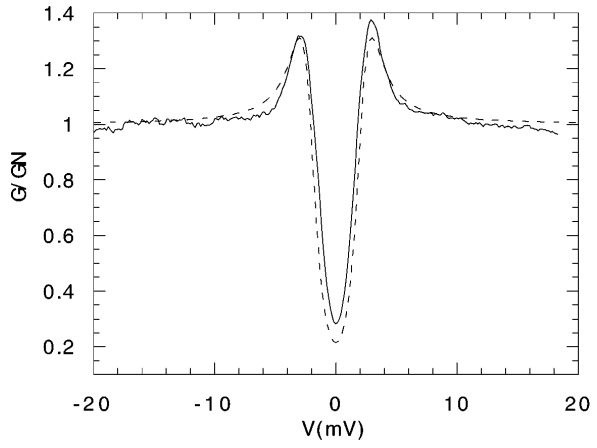

FIG. 1. Normalized experimental conductance spectrum recorded on $LuNi_2B_2C$ at 4.2 K (solid line) and calculated conductance spectrum using a smeared BCS density of states (dotted line). The parameters of the calculated curve are: $\Delta = 2.2$ meV and $\Gamma = 0.4$ meV.

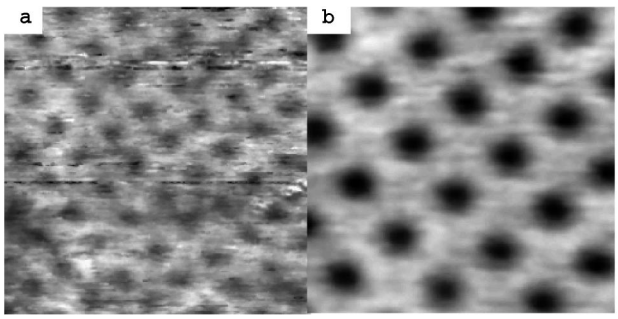

FIG. 2. (a) 2900 Å × 2900 Å conductance image (raw data) showing the square vortex lattice produced by a 1.5 T magnetic field in $LuNi_2B_2C$ at 4.2 K. (b) 1700 Å × 1700 Å conductance image after data processing (see text).

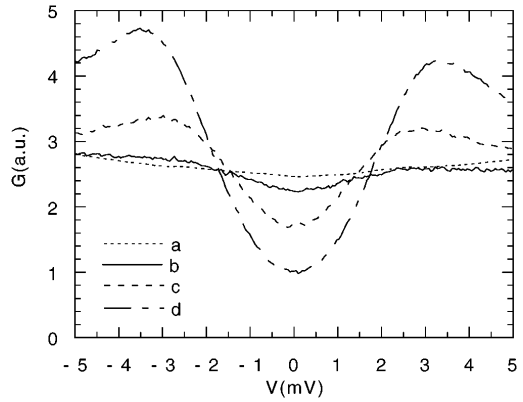

FIG. 3. dI/dV vs V for $LuNi_2B_2C$ at 4.2 K and 0.375 T recorded in the center of a vortex (a), and at 20 Å (b), 130 Å (c), 470 Å (d) from the center.

order of 115 Å. There is therefore significant scattering of quasiparticles within the confining vortex core diameter $2\xi = 2\sqrt{\frac{\Phi_0}{2\pi H_{c2}}} \approx 150$ Å which, together with thermal broadening effects at 4.2 K, may account for the observed absence of conductance peaks.

In order to explore the occurrence of a square VL we use a GL approach valid near T_c [29]. Since the energy difference between square and triangular VLs is very small [9,10], one can expect that a relatively small perturbation related to the crystalline symmetry in cubic and tetragonal superconductors can stabilize a square VL. The conventional GL theory is invariant with respect to arbitrary rotations and therefore does not contain any signature of the crystal symmetry. To account for the crystal symmetry, one has to keep higher order terms in the expansion of the energy with respect to the superconducting order parameter Ψ. The lowest order term, which breaks the circular symmetry and accounts for the square symmetry of the crystal near H_{c2}, has the form $|D_x^2\Psi|^2 + |D_y^2\Psi|^2$. Here $D_\alpha = \nabla_\alpha - \frac{2\pi i}{\Phi_0} A_\alpha$ is the gauge invariant derivative. The generalized energy functional $E[\Psi]$ for tetragonal superconductors can be written as

$$E[\Psi] = E_{\mathrm{GL}}[\Psi] + E_{\square}[\Psi], \tag{2}$$

where

$$E_{\mathrm{GL}}[\Psi] = \int d^3r \Big(-a_0|\tau|\,|\Psi|^2 + \frac{b_0}{2}\,|\Psi|^4 + a_0\xi_0^2|\mathbf{D}\Psi|^2 + \frac{B^2}{8\pi} \Big) \tag{3}$$

is the conventional GL term with standard notation and

$$E_{\square}[\Psi] = \varepsilon_{\square} a_0 \xi_0^4 \int d^3r (|D_x^2\Psi|^2 + |D_y^2\Psi|^2) \tag{4}$$

is the anisotropy term. The strength of the square anisotropy is determined by the dimensionless parameter $\varepsilon_{\square}$. The extra term induces an angular dependence of various quantities when the field is rotated in the xy plane. For example, the angular dependence of the upper critical field in the lowest order with respect to $\varepsilon_{\square}$ is

$$H_{c2}^{\parallel}(\phi) = H_{c2}^{\parallel}(0)\Big(1 + \frac{3\varepsilon_{\square}|\tau|}{16}(1 - \cos 4\phi)\Big), \tag{5}$$

where $\tau = (T - T_c)/T_c$ is the reduced temperature. This dependence can be used to evaluate $\varepsilon_{\square}$ experimentally.

We determine the equilibrium vortex configuration corresponding to the energy functionals in Eqs. (2)–(4) by minimizing the Abrikosov ratio $\beta = |\Psi|^4/(|\Psi|^2)^2$ [29]. The symmetry breaking part in the energy [Eq. (4)] stabilizes a square VL which, for $\varepsilon_{\square} < 0$, is oriented along the (110) crystal direction and, for $\varepsilon_{\square} > 0$, is oriented along the (100) direction. The isotropic part of the energy [Eq. (3)] induces the well-known hexagonal VL. The combination of both results in a distorted hexagonal VL, see Fig. 4. The distortion increases with increasing $|\varepsilon_{\square}|$ until a square VL becomes stable. This occurs in a second order phase transition at the phase boundary given by $\varepsilon_{\square}|\tau|\,\frac{8b^2}{9b-1} = -0.09$, where $b = H/H_{c2}$ (we assume $\varepsilon_{\square} < 0$). This boundary intersects the H_{c2} line at $\tau_{\mathrm{tr}} = 0.09/\varepsilon_{\square}$ (Fig. 4). The corresponding in-plane anisotropy $\Gamma_{45} = H_{c2}^{\parallel}(45°)/H_{c2}^{\parallel}(0)$ can be estimated using Eq. (5) as $\Gamma_{45} \approx 0.97$.

For the studied $LuNi_2B_2C$ single crystal, the temperature dependence of Γ_{45} has been systematically investigated by magnetization measurements [30]. We find an in-plane anisotropy of H_{c2} which increases monotonously with lowering T. The point $\Gamma_{45} \approx 0.97$, where the transition to the square VL is expected to occur, is reached at $T = 14$ K, implying $\varepsilon_{\square} \approx -0.8$. At this temperature, $H_{c2} \approx 0.6$ T for a field applied along the c axis. Based

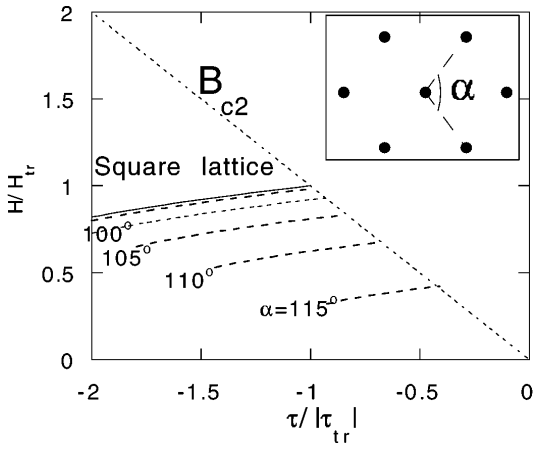

FIG. 4. Phase diagram for a tetragonal superconductor in the vicinity of the upper critical field. The reduced temperature $\tau = (T - T_c)/T_c$ is normalized to the square lattice transition temperature at H_{c2}, $\tau_{\mathrm{tr}} = 0.09/\varepsilon_{\square}$, and the field is normalized to the value of H_{c2} at this point. Contours of constant bond angle are also shown. The solid line corresponds to the second order phase transition line to a square VL. The inset shows the definition of the bond angle α.

on the phase diagram of Fig. 4, one would expect a square lattice at higher fields and lower temperatures, as we observed at 1.5 T and 4.5 K, where $\Gamma_{45} \approx 0.92$. The square lattice phase boundary shown in Fig. 4 is based on the lowest order fourfold correction to isotropic GL expression and cannot be extended to our low field experimental point at 4.5 K and 0.375 T. However, the stability of the square VL can be analyzed within London theory, which is expected to be valid sufficiently far from H_{c2}. An estimate of the relevant phenomenological parameters in terms of Fermi surface averages [31] suggests that the square lattice is stable for $LuNi_2B_2C$ above approximately 500 G, consistent with our STM observation.

In conclusion, STM measurements of the (001) surface of a $LuNi_2B_2C$ single crystal in zero magnetic field show a superconducting energy gap of 2.2 meV, which is remarkably constant over the sample surface and indicates weak coupling. In a magnetic field oriented along the (001) direction, we find a square VL oriented along the (110) crystalline direction. The square VL is correlated with an in-plane anisotropy $H_{c2}^{\parallel}(45°)/H_{c2}^{\parallel}(0) = 0.92$. The results are explained within the framework of the GL model in which higher order terms which reflect the square symmetry of the crystal are introduced in the expression for the free energy.

We thank P. L. Gammel for stimulating discussions and for providing his neutron diffraction data before publication. We are very grateful to D. G. Hinks who determined the orientation of our sample by x rays, to J. Zasadzinski for his comments, and to V. Vinokur for reviewing our manuscript. This work was supported by the NSF Science and Technology Center for Superconductivity under Contract No. DMR 91-20000 (Y. D. W., A. E. K., I. A.), by the US DOE Basic Energy Science-Material Science under Contract No. W-31-109-ENG-38 (M. I., U. W., V. M., G. W. C.) and Contract No. W-740-ENG-82 (P. C. C.).

*Permanent address: Dipartimento di Science Fisiche, Università di Napoli Federico II, Napoli, Italy.

†Permanent address: Department of Physics, Bar Ilan University, Ramat Gan, Israel.

[1] A. Moser, H. J. Hug, I. Parashikov, B. Stiefel, O. Fritz, H. Thomas, A. Baratoff, H. J. Güntherodt, and P. Chaudhari, Phys. Rev. Lett. **74**, 1847 (1995).

[2] H. Träuble and U. Essmann, J. Appl. Phys. **39**, 4052 (1968).

[3] U. Yaron, P. L. Gammel, A. P. Ramirez, D. A. Huse, D. J. Bishop, A. I. Goldman, C. Stassis, P. C. Canfield, K. Mortensen, and M. R. Eskildsen, Nature (London) **382**, 236 (1996).

[4] H. F. Hess, R. B. Robinson, R. C. Dynes, J. M. Valles, Jr., and J. V. Waszczak, Phys. Rev. Lett. **62**, 214 (1989).

[5] H. F. Hess, C. A. Murray, and J. V. Waszczak, Phys. Rev. Lett. **69**, 2138 (1992).

[6] Ch. Renner, A. D. Kent, Ph. Niedermann, and Ø. Fischer, Phys. Rev. Lett. **67**, 1650 (1991).

[7] S. Behler, S. H. Pan, P. Jess, A. Baratoff, H. J. Güntherodt, F. Lévy, G. Wirth, and J. Wiesner, Phys. Rev. Lett. **72**, 1750 (1994).

[8] I. Maggio-Aprile, Ch. Renner, A. Erb, E. Walker, and Ø. Fischer, Phys. Rev. Lett. **75**, 2754 (1995).

[9] A. A. Abrikosov, Sov. Phys. JETP **5**, 1174 (1957).

[10] W. H. Kleiner, L. M. Roth, and S. H. Autler, Phys. Rev. **133**, 1226 (1964).

[11] See C. A. Bolle, F. De La Cruz, P. L. Gammel, J. V. Waszczak, and D. J. Bishop, Phys. Rev. Lett. **71**, 4039 (1993), and references therein.

[12] B. Keimer, W. Y. Shih, R. W. Erwin, J. W. Lynn, F. Dogan, and I. A. Aksay, Phys. Rev. Lett. **73**, 3459 (1994).

[13] E. H. Brandt and U. Essmann, Phys. Status Solidi (b) **144**, 13 (1987).

[14] B. Obst, Phys. Lett. **28A**, 662 (1969).

[15] *Anisotropy Effects in Superconductors*, edited by H. Weber (Plenum, New York, 1977); D. K. Christen *et al.*, Physica (Amsterdam) **135B**, 369 (1985).

[16] B. Obst and E. H. Brandt, Phys. Lett. **64A**, 460 (1978).

[17] L. Kramer, Phys. Rev. B **3**, 3821 (1971).

[18] P. L. Gammel (to be published).

[19] R. J. Cava, H. Takagi, H. W. Zandbergen, J. J. Krajeski, W. F. Peck, Jr., T. Siegrist, B. Batlogg, B. van Dover, R. J. Felder, K. Mizuhaski, J. O. Lee, H. Eisaki, and S. Uchida, Nature (London) **367**, 252 (1994).

[20] R. Nagarajan, C. Mazumdar, Z. Hossain, S. K. Dhar, K. V. Gopalakrishnan, L. C. Gupta, C. Godart, B. D. Padalia, and R. Vijayraghavan, Phys. Rev. Lett. **72**, 274 (1994).

[21] T. Siegrist, H. W. Zandbergen, R. J. Cava, J. J. Krajewski, and W. F. Peck, Jr., Nature (London) **367**, 254 (1994).

[22] B. K. Cho, P. C. Canfield, and D. C. Johnston, Phys. Rev. B **52**, R3844 (1995).

[23] P. L. Gammel (private communication).

[24] E. L. Wolf, *Principles of Electron Tunneling Spectroscopy* (Oxford University Press, New York, 1985).

[25] R. C. Dynes, V. Narayanamurti, and J. P. Garno, Phys. Rev. Lett. **41**, 1509 (1978).

[26] Toshikazu Ekino *et al.*, Phys. Rev. B **53**, 5640 (1996); G. T. Jeong *et al.*, Physica (Amsterdam) **253C**, 48 (1995); T. Hasegawa *et al.*, Physica (Amsterdam) **235C-240C**, 1859 (1994).

[27] P. L. Gammel (unpublished).

[28] K. D. D. Rathnayaka, D. G. Naugle, B. K. Cho, and P. C. Canfield, Phys. Rev. B **53**, 5688 (1996).

[29] A. E. Koshelev and I. Aranson (to be published).

[30] V. Metlushko, U. Welp, A. E. Koshelev, I. Aranson, G. W. Crabtree, and P. C. Canfield (to be published).

[31] V. Kogan, P. L. Gammel, and D. J. Bishop, Phys. Rev. B **55**, R8693 (1997).